In Vitro Cell.Dev.Biol.—Animal (2017) 53:744–751
DOI 10.1007/s11626-017-0178-6

The influence of simulated microgravity on proliferation and apoptosis in U251 glioma cells

Jiao Zhao[1] · He Ma[2] · Leitao Wu[1] · Liang Cao[1] · Qianqian Yang[2] · Haijun Dong[1] · Zongren Wang[1] · Jing Ma[1] · Zhen Li[2]

Received: 15 January 2017 / Accepted: 7 June 2017 / Published online: 13 July 2017 / Editor: Tetsuji Okamoto

Abstract Several studies have indicated that microgravity can influence cellular progression, proliferation, and apoptosis in tumor cell lines. In this study, we observed that simulated microgravity inhibited proliferation and induced apoptosis in U251 malignant glioma (U251MG) cells. Furthermore, expression of the apoptosis-associated proteins, p21 and insulin-like growth factor binding protein-2 (IGFBP-2), was upregulated and downregulated, respectively, following exposure to simulated microgravity. These findings indicate that simulated microgravity inhibits proliferation while inducing apoptosis of U251MG cells. The associated effects appear to be mediated by inhibition of IGFBP-2 expression and stimulation of p21 expression. This suggests that simulated microgravity might represent a promising method to discover new targets for glioma therapeutic strategy.

Keywords Simulated microgravity · Malignant glioma · Apoptosis · P21 · IGFBP-2

Jiao Zhao and He Ma contributed equally to this work.

✉ Jing Ma
jingma@fmmu.edu.cn

✉ Zhen Li
lizhenhe@fmmu.edu.cn

[1] Department of Traditional Chinese Medicine, Xijing Hospital, Fourth Military Medical University, Xi'an, Shaanxi, China

[2] Department of Histology and Embryology, Fourth Military Medical University, Xi'an, Shaanxi, China

Introduction

Malignant gliomas represent the most common and aggressive type of primary brain tumor in adults. These tumors are characterized by rapid growth, extensive invasiveness, and angiogenesis (Wen and Kesari 2008). Malignant gliomas account for approximately 70% of the 22,500 new cases of malignant primary brain tumors diagnosed in adults in the USA each year (Paw et al. 2015). Despite multimodality therapies including aggressive surgery combined with radiation, chemotherapy, and biological therapy, median survival for patients with high-grade gliomas is frequently less than 2 yr (Komotar et al. 2008). Mounting evidence suggests that resistance to apoptosis leads to the sustained survival of malignant glioma cells (Li et al. 2009). Thus, more effective pro-apoptotic interventions are urgently required to improve the treatment of this malignancy.

Several studies performed on astronauts have shown that space flight results in profound changes in multiple organs and systems, causing detrimental health effects including muscular atrophy, osteopenia or bone loss, and decreased immune functions (Petersen et al. 2017; Van Ombergen et al. 2017). Moreover, a growing number of studies have reported the significant effect of spaceflight microgravity on cell lines, primary cell, stem cell, and whole animals (Meloni et al. 2011; Bailey et al. 2014; Blaber et al. 2014;). Access to flight is costly, and the opportunities are scarce, resulting in numerous experiments simulating the real weightless condition having been performed, although the biological responses in microgravity simulators are not completely identical to those of real microgravity experiments (Herranz et al. 2013). In addition to the physiological effects in spaceflight, an increasing number of simulated studies have indicated that microgravity has evident effects on major cellular events, namely cell cycle progression, proliferation, differentiation, and apoptosis,

especially in tumor cells such as gastric carcinoma cell and seminoma cell (Ferranti et al. 2014; Jhala et al. 2014; Zhu et al. 2014). Conversely, relatively little work has been conducted on the effects of microgravity on glioma cells, although it has been reported that microgravity induces apoptosis in rat C_6 glioma cells (Uva et al. 2002) while inhibiting proliferation and migration in human glioma cells (Takeda et al. 2009; Shi et al. 2015). Moreover, the underlying mechanisms pertaining to the effects of microgravity on glioma cells are still unclear.

The mutation of tumor suppressor gene, *p53*, occurs frequently in human gliomas (Frankel et al. 1992). Thus, it is pivotal to find a *p53*-independent method to treat malignant gliomas. In this study, a U251MG glioma cell line harboring mutant *p53* was utilized as an experimental model for malignant glioma. We applied a clinostat to generate a microgravity environment to investigate the effects of simulated microgravity on the proliferation and apoptosis of U251MG cells and the possible involved mechanism.

Materials and Methods

Cell culture U251MG cells were obtained from the American Type Culture Collection (San Francisco, CA). Cells were cultured in high-glucose DMEM (Gibco; Thornwood, NY) supplemented with 10% fetal bovine serum (Gibco), penicillin (100 U/mL), and streptomycin (100 μg/mL) at 37°C in an atmosphere containing 5% CO_2.

Simulation of microgravity conditions The 2D clinostat system is an effective, ground-based tool that is used to simulate microgravity. Details pertaining to the application of this method have been previously described elsewhere (Wang et al. 2013). Briefly, U251MG cells were seeded at a density of 1×10^5 cells on 2.5 cm × 2.5 cm coverslips. After the cells were allowed to grow for 8 h, the coverslips were inserted into fixtures in the chambers, which were subsequently filled with high-glucose DMEM. The chambers were randomized for stationary control without rotation and clinorotation (1 G group) or cultured under simulated microgravity conditions (10^{-3} G group). The clinostat was positioned in an incubator at 37°C.

Cell proliferation assay The effect of simulated microgravity on U251MG cell proliferation was measured using a Cell Counting Kit-8 (CCK-8) assay kit (Dojindo; Kumamoto, Japan) with the standard protocol. The absorbance was measured at an optical density (OD) of 450 nm using a Sunrise Microplate Reader (Tecan Group Ltd.; Männedorf, Switzerland).

TUNEL assay Terminal deoxynucleotidyl transferase-mediated dUTP nick-end labeling (TUNEL) was conducted using a TUNEL apoptosis detection kit (Roche; Pleasanton, CA) for DNA fragmentation fluorescence staining according to the manufacturer's protocol. The sections were mounted and viewed using a fluorescence microscope (Olympus; Tokyo, Japan).

Transmission electron microscopy analysis Cells were fixed in ice-cold 2.5% glutaraldehyde in PBS (pH 7.3) for 4 h, postfixed in 1% osmium tetroxide with 0.1% potassium ferricyanide, and dehydrated in a graded series of ethanol (30–90%). The cells were subsequently embedded in Epon (Energy Beam Sciences; Agawam, MA). Ultrathin sections (65 nm) were examined under a Tecnai G2 Polara Cryo-TEM (FEI; Hillsboro, OR).

Human Apoptosis Antibody Array The relative levels of 43 apoptosis-related proteins were simultaneously detected in cell lysates using a RayBio Human Apoptosis Antibody Array Kit (RayBiotech; Norcross, GA) according to the manufacturer's instructions. Briefly, U251MG cells from different groups were lysed, and the total proteins were purified. The protein concentration was determined using a BCA Protein Assay Kit (Thermo Fisher Scientific; Waltham, MA). A total of 35 μg of protein extract was hybridized with human apoptosis glass slide subarrays overnight at 4°C and incubated with biotin-conjugated primary antibodies for 2 h at room temperature. Then, the glass slides were washed and incubated with fluorescence-conjugated streptavidin secondary antibodies. The signals were visualized by an Axon GenePix 4000B Microarray Scanner (Axon Instruments; Union City, CA), and the densities of the resultant spots were analyzed using AAH-APO-G1 software (RayBiotech).

Real-time RT-PCR analysis Total RNA was extracted from U251MG cells using TRIzol reagent (Invitrogen; Carlsbad, CA). Real-time PCR was performed on an ABI PRISM 7900 Real-Time PCR System (Applied Biosystems; Foster City, CA) using SYBR Green and ROX (Takara; Shiga, Japan) as reference dyes. The primer sequences that were utilized were as follows: *p21*, 5′-ggcagaccatgtggacctgt-3′ and 5′-ggagtttggagtggtagaaa-3′; *IGFBP-2*, 5′-catcaagtcgggtatgaagg-3′ and 5′-acctggtccagttcctgttg-3′. Human *β-actin* was used as the internal controls. Quantitative data were expressed by normalizing the densitometric units to β-actin.

Western blot analysis Control and simulated microgravity-grown cells were harvested and lysed with RIPA buffer for 30 min on ice. Then, the cell lysis buffers were centrifuged, and the protein concentrations (from resultant supernatants) were determined using a BCA protein assay (Thermo Fisher Scientific). Proteins of a total content of 25 μg were separated by NuPAGE Bis-Tris gel electrophoresis and transferred onto a PVDF membrane. The membrane was incubated with

primary antibodies against IGFBP-2, p21, and β-actin (CST; Danvers, MA), respectively, and with horseradish peroxidase-conjugated secondary antibody (Santa Cruz Biotechnology; Santa Cruz, CA). Specific protein bands were subsequently visualized using an enhanced chemiluminescence system according to the manufacturer's instructions.

Statistical analysis Results are expressed as the mean ± SD of three or more independent biological samples. Statistical analyses to assess significant differences were performed using one-way ANOVA (using GraphPad Prism 5 software, GraphPad Prism Software Inc.; San Diego, CA). $p < 0.05$ was considered statistically significant. In all graphs, the asterisk indicates significant difference.

Results

Effect of simulated microgravity on U251MG cell proliferation The CCK-8 method was applied to detect cell proliferation. Figure 1 shows that compared to the control group, the OD value was significantly decreased in microgravity-treated groups ($p < 0.05$). Moreover, following treatment with microgravity (10^{-3} G) for 12, 24, 48, and 72 h, the inhibitory rates were 83.6 ± 0.37, 33.3 ± 0.4, 21.4 ± 0.28, and 16.62 ± 0.35%, respectively. These results suggest that the extent of the simulated microgravity effect was time-dependent.

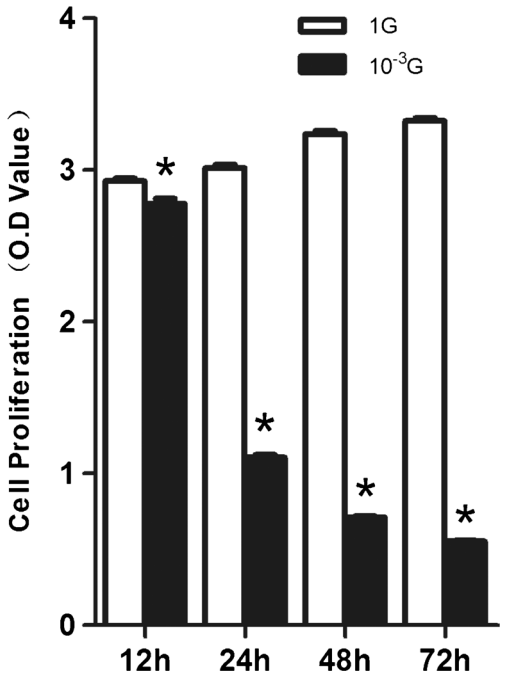

Figure 1. Cell proliferation in simulated microgravity and standard culture groups. U251MG cells were examined by the CCK-8 assay following 12 to 72 h of culture. The data were presented as means ± SD from three independent experiments. *$p < 0.05$ vs. standard gravity group.

Effect of simulated microgravity on apoptosis of U251MG cells A TUNEL assay and a flow cytometry analysis were conducted to examine the effect of simulated microgravity on U251MG cellular apoptosis. TUNEL staining revealed intensely green fluorescent nuclei, which predominantly occurred in the simulated microgravity groups. Limited staining was observed in the standard gravity group. DAPI staining (blue fluorescence) was also utilized to eliminate the possibility that a reduction in TUNEL staining may have been caused by the absence of nuclei (Fig. 2*A*). Data pertaining to the cellular apoptotic rate was measured for each group using flow cytometry (Fig. 2*B*). The apoptotic rates of U251MG cells were 28.9 ± 1.2, 40 ± 0.98, 39.2 ± 1.46, and 71.2 ± 1.33% after simulated microgravity (10^{-3} G) treatment for 12, 24, 48, and 72 h, respectively. These values were significantly higher than those for the control group (8.8 ± 0.74%) ($p < 0.05$).

Alterations in cell ultrastructure following transmission electron microscopy analysis To determine further the pro-apoptotic effects of simulated microgravity on U251MG cells, TEM was used to monitor changes in cellular ultrastructure in clinorotation and control cells. The electron microscope images reveal the presence of edge-clustered nuclear membranes (arrows) with swollen or disrupted organelles (asterisks) following 72 h of treatment (Fig. 2*C1*, *C2*). However, the control group contained regular nuclei and evenly distributed chromatin (Fig. 2*C3*, *C4*).

Apoptosis array analysis To explore the molecular mechanisms that underpin apoptosis in clinorotation cells, we used a Human Apoptosis Antibody Array Kit to investigate the effect of simulated microgravity on 44 apoptosis-related proteins. Our results indicated that six (caspase-8, IGFBP-4, IGFBP-2, p21, p53, and TRAILR-2) of the 44 proteins included in the array exhibited changes. Following a combinatorial analysis that assessed signal value size, fold change, and *t* test, p21 and IGFBP-2 were shown to be the two most differentially expressed proteins, while the expression changes for the other four proteins were not statistically significant. Array data pertaining to p21 and IGFBP-2 are indicated by a red and yellow box, respectively (Fig. 3).

Real-time PCR and western blot analysis of p21 and IGFBP-2 expression in response to simulated microgravity The expression profiles for p21 and IGFBP-2 messenger RNA (mRNA) are shown in Fig. 4*A*. It is evident that p21 mRNA expression increased, whereas IGFBP-2 mRNA decreased in the simulated microgravity (10^{-3} G) group compared with that in the control group ($p < 0.05$). Following

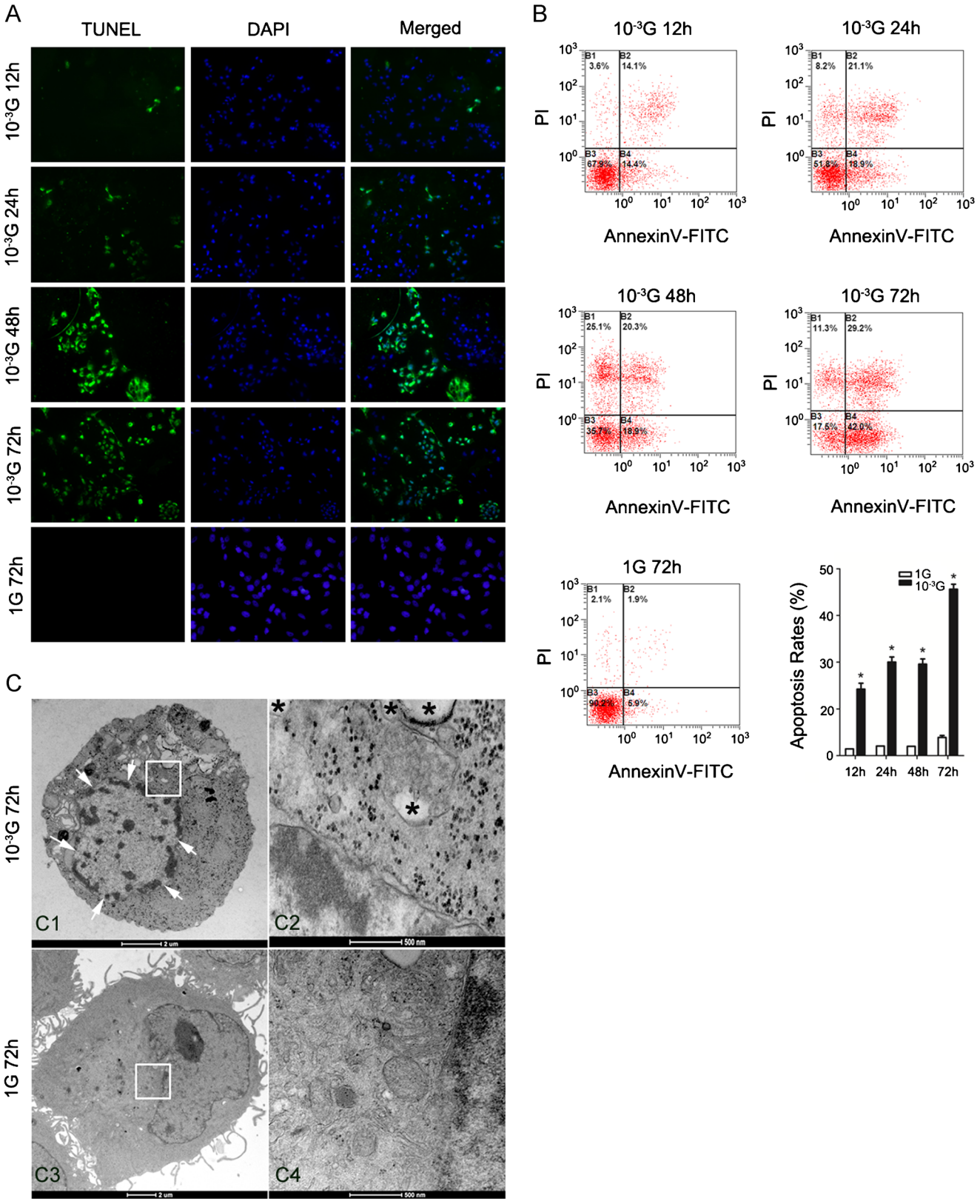

exposure to the longest simulated microgravity treatment time, p21 mRNA expression was observed to increase gradually, whereas IGFBP-2 mRNA expression gradually decreased ($p < 0.05$). Figure 4*B*, *C* shows that p21 protein expression was increased in the clinorotation group compared to the control group, whereas IGFBP-2 protein expression was

◀ **Figure 2.** Induction of apoptosis in U251MG cells by simulated microgravity. (*A*) Cells were exposed to simulated microgravity (10^{-3} G) or standard gravity (1 G) for different time periods. TUNEL-positive cells appear *green*, while DAPI staining (*blue fluorescence*) indicates the position of nuclei (overall magnification of ~×200). (*B*) Apoptosis was analyzed by FACS using the Annexin V-FITC detection kit. The apoptosis rates were statistically evaluated. The data were presented as means ± SD from three independent experiments. *$p < 0.05$ vs. standard gravity group. (*C*) Changes in the ultrastructure of U251MG cells following simulated microgravity treatment. Cells cultured under simulated microgravity (10^{-3} G) for 72 h (*C1*), enlarged cellular image corresponding to the area indicated by the *white square* in *C1* (*C2*), control cells (*C3*), and enlarged cellular image corresponding to the area indicated by the *white square* in *C3* (*C4*). Compared with control cells, clinorotation cells exhibited morphological features of apoptosis, including edge-clustered nuclear membranes (*arrows*), swollen or disrupted organelles (*asterisks*), and loss of plasma membranes.

relatively lower in the clinorotation group ($p < 0.05$). p21 protein expression gradually increased following exposure to increased treatment times, whereas IGFBP-2 protein expression gradually decreased ($p < 0.05$). Western blot analyses further confirmed a time-dependent expression effect following exposure to simulated microgravity. These results were compatible with the results of the mRNA expression analysis.

Discussion

Several reports have shown that microgravity can affect cell proliferation and apoptosis in various tumor cell lines including glioma cells (Uva et al. 2002; Jhala et al. 2014). However, the underlying mechanisms that underpin the proliferation and apoptosis effects pertaining to simulated microgravity in glioma are still unclear. In this study, we observed that simulated microgravity inhibited proliferation while inducing apoptosis in U251MG cells. Moreover, we demonstrated for the first time the potential molecular mechanisms that underpin the effects mediated by simulated microgravity on U251MG cells. These effects occurred concomitantly with the upregulation of p21 and the downregulation of IGFBP-2. It is likely that alterations in the expression of p21 and IGFBP-2 could contribute to apoptosis and proliferation inhibition following exposure to microgravity.

However, microgravity-specific effects pertaining to cell proliferation have been shown to depend on the cell type analyzed (Lin et al. 2016). Multiple studies have shown that microgravity suppresses cell proliferation in tumor cells including mammalian osteosarcoma cells (Wei et al. 2013) and human breast cancer cells (Vassy et al. 2003). In this study, we observed a significant time-dependent reduction in the OD value of U251MG cells compared to the control group. This suggests that simulated microgravity inhibits the proliferation of U251MG cells. Our results are consistent with a previous study, which reported that simulated microgravity inhibited cell proliferation in malignant glioma cell lines (Takeda et al. 2009). Cell cycle arrest induced by microgravity is partially caused by the inhibition of cell proliferation. Nevertheless, the results of studies pertaining to cell cycle arrest under microgravity are still contentious. Coinu et al. observed that modeled microgravity induced partial arrest in the G2/M phase in vascular smooth muscle cells and neoplastic human breast cancer cells (Coinu et al. 2006). However, in U251MG, Takeda et al. observed that simulated microgravity did not precipitate any significant changes in the cell cycle. What is more, they also reported a reduction in mitochondrial activity and speculated that this occurrence might stall cell cycle progression, thereby inhibiting cell proliferation instead of affecting specific cell cycle check points (Takeda et al. 2009).

Recent studies have reported that microgravity induces apoptosis in most cell lines and tissues (Pietsch et al. 2011). As part of this analysis, we performed a TUNEL assay and found that the apoptotic rates of U251MG cells were significantly increased following exposure to simulated microgravity. In addition, a series of ultrastructure events including edge-clustered nuclear membranes and swollen or disrupted organelles were observed by TEM. Similarly, Uva et al. also observed transient apoptosis in rat C_6 glioma cells following conventional epifluorescence microscopy and TUNEL staining (Uva et al. 2002). A recent report by Wang et al. demonstrated that the morphology and cell cytoskeleton system of human glioma cells were significantly modified by simulated microgravity. They also reported an elevated cellular apoptosis rate and hypothesized that the rearrangement of the cytoskeleton caused human glioma cellular apoptosis (Wang et al. 2016).

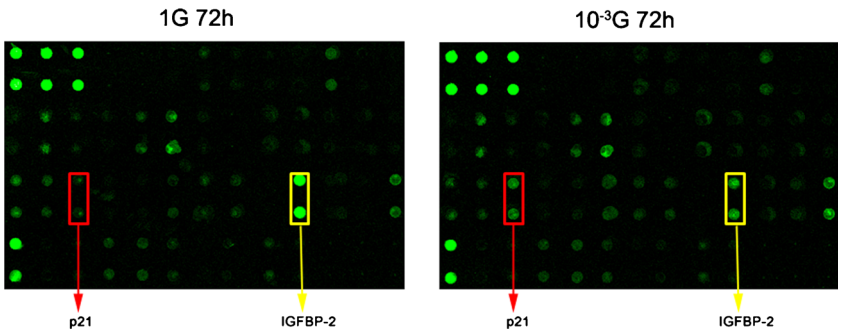

Figure 3. Screening of apoptosis factors associated with simulated microgravity treatment in U251MG cells. Cells were cultured under simulated microgravity (10^{-3} G) or standard gravity (1 G) for 72 h and subjected to apoptosis factor antibody array analysis. *p21*-specific and *IGFBP-2*-specific data are indicated.

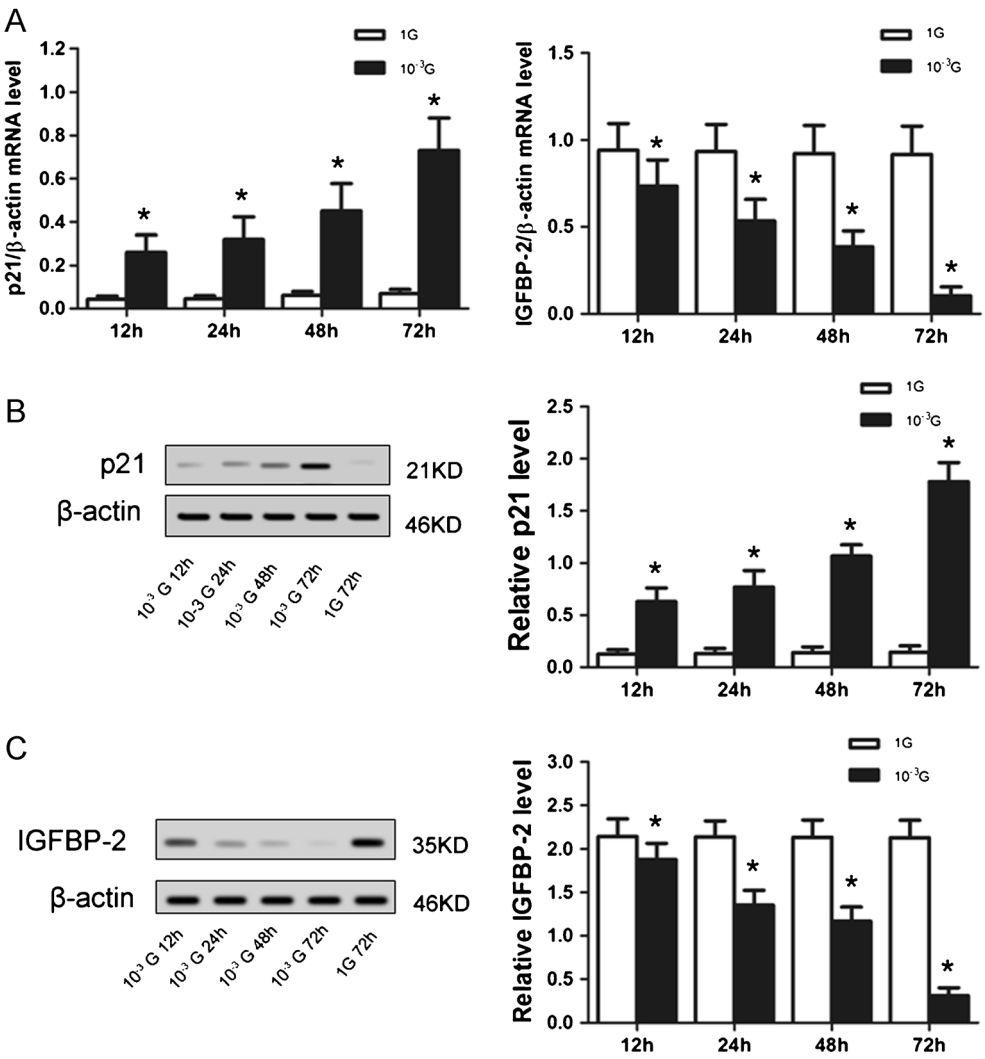

Figure 4. mRNA and protein expression of p21 and IGFBP-2 in U251MG cells. Real-time RT-PCR and western blot analysis were performed after U251MG cells were cultured under standard gravity (1 G) or simulated microgravity (10^{-3} G) conditions for different time periods. (*A*) The *bar graph* shows the ratios of p21 (*left panel*) and IGFBP-2 (*right panel*) mRNA relative to the amount of *β-actin* mRNA. The western blot images of *p21* and *IGFBP-2* are, respectively, shown in (*B*, *left panel*) and (*C*, *left panel*). The *right panels* represent the densitometric analysis of the data. β-Actin was used as a loading control. Data are expressed as mean ± SD ($n = 6$). *$p < 0.01$ vs. the standard gravity (1 G) group.

To investigate the mechanisms that underlie the proliferation inhibition and apoptosis effects pertaining to U251MG following exposure to simulated microgravity, we conducted a human apoptosis antibody array analysis. This analysis indicated that p21 and IGFBP-2 were the two most differentially expressed proteins, while the changes in expression of other apoptosis-associated proteins including caspase-8, p53, and TRAILR-2 were not significant. This suggests that p21 and IGFBP-2 are involved in simulated gravity-induced U251MG cellular apoptosis. The cyclin-dependent kinase (CDK) inhibitor, p21, has multiple roles including cell cycle regulation, differentiation, apoptosis, and transcriptional regulation after DNA damage (Karimian et al. 2016). In addition, several studies have shown that p21 plays a key role in carcinogenesis and tumor growth promotion (Prives and Gottifredi 2008). Indeed, the role of p21 might be regulated by the status of p21 itself and/or the differences in the histological types of cancers that have been analyzed (Xia et al. 2011). We examined the expression of p21 using real-time PCR and western blot analysis and confirmed that simulated microgravity stimulated the expression of p21 in U251MG cells. Dong et al. reported that small double-stranded RNA (dsRNA) mediated overexpression of p21 in human glioma SHG-44 cells promotes cell cycle arrest and enhances apoptosis (Dong et al. 2014). In addition, Dai et al. reported that the downregulation of p21 promoted by the overexpression of lysine-specific demethylase 5B (KDM5B) stimulates glioma cell growth (Dai et al. 2014). Thus, p21 is likely to act as a tumor suppressor in human glioma cell lines, and in our study, apoptosis of U251MG cells may have been induced by the upregulation of p21. Simulated microgravity did not affect specific cell cycle check points in U251MG (Takeda et al. 2009); therefore, we deduce that p21 upregulation leads to apoptosis rather than cell cycle arrest in this cell line. p53 is considered the main transcriptional regulator of p21. However, p21 can also be induced independently of p53 by other transcription factors including breast cancer susceptibility gene 1 (BRCA1), TGF-β, and double homeobox 4 (Dux4) (Mullan et al. 2006; Meng et al. 2013; Xu et al. 2014). Indeed, p53-independent regulation of p21 has been reported in several human tumor

cell lines including human glioma cells (Miyata et al. 2013; Fang et al. 2016). As the U251MG cell line is a p53 mutant, our findings also suggest that the expression of p21 is induced by simulated microgravity through a p53-independent pathway. Insulin-like growth factor binding protein-2 (IGFBP-2) is conventionally known to modulate IGF signaling and is produced by a variety of different tissues via complex regulatory processes (Firth and Baxter 2002). Emerging evidence suggests that IGFBP-2 plays additional roles in tumor biology via IGF-independent mechanisms, and the role of IGFBP-2 is dependent on cell type and cellular microenvironments (Pickard and McCance 2015). In human glioma cells, IGFBP-2 is one of the most consistently overexpressed factors, especially in high-grade glioma patients (Lin et al. 2009). Therefore, IGFBP-2 is considered a valuable biomarker for glioma patient prognosis (McDonald et al. 2007). Moreover, the overexpression of IGFBP-2 induces cellular proliferation and invasion, while also stimulating tumor-grade progression in glioma (Han et al. 2014). Thus, in this study, we analyzed IGFBP-2 expression changes using real-time PCR and western blot analyses and observed that simulated microgravity inhibited the expression of IGFBP-2. Recent studies have shown that the downregulation of IGFBP-2 could inhibit proliferation of glioma cells. Phillips et al. found that the continued expression of IGFBP-2 is required for glioma maintenance as inhibition of IGFBP-2 has been observed to block progression (Phillips et al. 2016). Patil et al. reported that IGFBP-2 or its C-terminal domain could lead to glioma growth (Patil et al. 2016). Taken together, these results show that simulated microgravity inhibits U251MG cell proliferation by downregulating IGFBP-2. However, the effect of simulated microgravity on cells could not be permanent, and the cells would recover to basal status after return to normal condition (Silvano et al. 2015), which indicates that simulated microgravity could not be an available therapy at present, but it might be a method to discover new targets for potential development into a treatment on glioma. Moreover, it should be noted that comparing with the typical glioblastoma, long-term cultures of U251MG displayed variations in genotype and phenotype and showed an increased growth rate in vitro (Torsvik et al. 2014). Therefore, results in this study only represent the proprieties of a U251MG subclone under simulated microgravity, and the whole glioma tissue should be investigated under simulated microgravity in further studies. The limitation of this study is that it is still unclear how simulated microgravity mediates alterations in p21 and IGFBP-2 expression. Further studies are required to elucidate the associated mechanisms.

In conclusion, our study demonstrates that simulated microgravity inhibits proliferation and induces U251MG cellular apoptosis. These effects are at least partially due to the microgravity-induced downregulation of IGFBP-2 and upregulation of p21. Thus, we propose that simulated microgravity might be an effective method to discover new targets for glioma therapeutic strategy.

Acknowledgements This work was supported by the National Natural Science Foundation of China (No. 81273879). We thank Dr. Wen-dong Bai, Dr. Chu-chao Zhu, Dr. Yuan Xing, and Dr. Lu Wang for their expert technical assistance.

References

Bailey JF, Hargens AR, Cheng KK, Lotz JC (2014) Effect of microgravity on the biomechanical properties of lumbar and caudal intervertebral discs in mice. J Biomech 47:2983–2988

Blaber E, Sato K, Almeida EA (2014) Stem cell health and tissue regeneration in microgravity. Stem Cells Dev 23(Suppl 1):73–78

Coinu R, Chiaviello A, Galleri G, Franconi F, Crescenzi E, Palumbo G (2006) Exposure to modeled microgravity induces metabolic idleness in malignant human MCF-7 and normal murine VSMC cells. FEBS Lett 580:2465–2470

Dai B, Hu Z, Huang H, Zhu G, Xiao Z, Wan W, Zhang P, Jia W, Zhang L (2014) Overexpressed KDM5B is associated with the progression of glioma and promotes glioma cell growth via downregulating p21. Biochem Biophys Res Commun 454:221–227

Dong Z, Dang Y, Chen Y (2014) Small double-stranded RNA mediates the anti-cancer effects of p21WAF1/ClP1 transcriptional activation in a human glioma cell line. Yonsei Med J 55:324–330

Fang L, Cheng Q, Zhao J, Ge Y, Zhu Q, Zhao M, Zhang J, Zhang Q, Li L, Liu J, Zheng J (2016) A p53-independent apoptotic mechanism of adenoviral mutant E1A was involved in its selective antitumor activity for human cancer. Oncotarget. doi:10.18632/oncotarget.10221

Ferranti F, Caruso M, Cammarota M, Masiello MG, Corano Scheri K, Fabrizi C, Fumagalli L, Schiraldi C, Cucina A, Catizone A, Ricci G (2014) Cytoskeleton modifications and autophagy induction in TCam-2 seminoma cells exposed to simulated microgravity. Biomed Res Int 2014:904396

Firth SM, Baxter RC (2002) Cellular actions of the insulin-like growth factor binding proteins. Endocr Rev 23:824–854

Frankel RH, Bayona W, Koslow M, Newcomb EW (1992) p53 mutations in human malignant gliomas: comparison of loss of heterozygosity with mutation frequency. Cancer Res 52:1427–1433

Han S, Li Z, Master LM, Master ZW, Wu A (2014) Exogenous IGFBP-2 promotes proliferation, invasion, and chemoresistance to temozolomide in glioma cells via the integrin beta1-ERK pathway. Br J Cancer 111:1400–1409

Herranz R, Anken R, Boonstra J, Braun M, Christianen PC, de Geest M, Hauslage J, Hilbig R, Hill RJ, Lebert M, Medina FJ, Vagt N, Ullrich O, van Loon JJ, Hemmersbach R (2013) Ground-based facilities for simulation of microgravity: organism-specific recommendations for their use, and recommended terminology. Astrobiology 13:1–17

Jhala DV, Kale RK, Singh RP (2014) Microgravity alters cancer growth and progression. Curr Cancer Drug Targets 14:394–406

Karimian A, Ahmadi Y, Yousefi B (2016) Multiple functions of p21 in cell cycle, apoptosis and transcriptional regulation after DNA damage. DNA Repair (Amst) 42:63–71

Komotar RJ, Otten ML, Moise G, Connolly ES Jr (2008) Radiotherapy plus concomitant and adjuvant temozolomide for glioblastoma—a critical review. Clin Med Oncol 2:421–422

Li J, Zhang S, Chen J, Du T, Wang Y, Wang Z (2009) Modeled microgravity causes changes in the cytoskeleton and focal adhesions, and decreases in migration in malignant human MCF-7 cells. Protoplasma 238:23–33

Lin SC, Gou GH, Hsia CW, Ho CW, Huang KL, Wu YF, Lee SY, Chen YH (2016) Simulated microgravity disrupts cytoskeleton

organization and increases apoptosis of rat neural crest stem cells via upregulating CXCR4 expression and RhoA-ROCK1-p38 MAPK-p53 signaling. Stem Cells Dev 25:1172–1193

Lin Y, Jiang T, Zhou K, Xu L, Chen B, Li G, Qiu X, Jiang T, Zhang W, Song SW (2009) Plasma IGFBP-2 levels predict clinical outcomes of patients with high-grade gliomas. Neuro-Oncology 11:468–476

McDonald KL, O'Sullivan MG, Parkinson JF, Shaw JM, Payne CA, Brewer JM, Young L, Reader DJ, Wheeler HT, Cook RJ, Biggs MT, Little NS, Teo C, Stone G, Robinson BG (2007) IQGAP1 and IGFBP2: valuable biomarkers for determining prognosis in glioma patients. J Neuropathol Exp Neurol 66:405–417

Meloni MA, Galleri G, Pani G, Saba A, Pippia P, Cogoli-Greuter M (2011) Space flight affects motility and cytoskeletal structures in human monocyte cell line J-111. Cytoskeleton 68:125–137

Meng XM, Chung AC, Lan HY (2013) Role of the TGF-beta/BMP-7/Smad pathways in renal diseases. Clin Sci (Lond) 124:243–254

Miyata S, Urabe M, Gomi A, Nagai M, Yamaguchi T, Tsukahara T, Mizukami H, Kume A, Ozawa K, Watanabe E (2013) An R132H mutation in isocitrate dehydrogenase 1 enhances p21 expression and inhibits phosphorylation of retinoblastoma protein in glioma cells. Neurol Med Chir (Tokyo) 53:645–654

Mullan PB, Quinn JE, Harkin DP (2006) The role of BRCA1 in transcriptional regulation and cell cycle control. Oncogene 25:5854–5863

Patil SS, Gokulnath P, Bashir M, Shwetha SD, Jaiswal J, Shastry AH, Arimappamagan A, Santosh V, Kondaiah P (2016) Insulin-like growth factor binding protein-2 regulates beta-catenin signaling pathway in glioma cells and contributes to poor patient prognosis. Neuro-Oncology 18:1487–1497

Paw I, Carpenter RC, Watabe K, Debinski W, Lo HW (2015) Mechanisms regulating glioma invasion. Cancer Lett 362:1–7

Petersen N, Lambrecht G, Scott J, Hirsch N, Stokes M, Mester J (2017) Postflight reconditioning for European astronauts—a case report of recovery after six months in space. Musculoskelet Sci Pract 27(Suppl 1):S23–S31

Phillips LM, Zhou X, Cogdell DE, Chua CY, Huisinga A, Hess KR, Fuller GN, Zhang W (2016) Glioma progression is mediated by an addiction to aberrant IGFBP2 expression and can be blocked using anti-IGFBP2 strategies. J Pathol 239:355–364

Pickard A, McCance DJ (2015) IGF-binding protein 2—oncogene or tumor suppressor? Front Endocrinol 6:25

Pietsch J, Bauer J, Egli M, Infanger M, Wise P, Ulbrich C, Grimm D (2011) The effects of weightlessness on the human organism and mammalian cells. Curr Mol Med 11:350–364

Prives C, Gottifredi V (2008) The p21 and PCNA partnership: a new twist for an old plot. Cell Cycle 7:3840–3846

Shi ZX, Rao W, Wang H, Wang ND, Si JW, Zhao J, Li JC, Wang ZR (2015) Modeled microgravity suppressed invasion and migration of human glioblastoma U87 cells through downregulating store-operated calcium entry. Biochem Biophys Res Commun 457:378–384

Silvano M, Miele E, Valerio M, Casadei L, Begalli F, Campese AF, Besharat ZM, Alfano V, Abballe L, Catanzaro G (2015) Consequences of simulated microgravity in neural stem cells: biological effects and metabolic response. J Stem Cell Res Ther 5:289–296

Takeda M, Magaki T, Okazaki T, Kawahara Y, Manabe T, Yuge L, Kurisu K (2009) Effects of simulated microgravity on proliferation and chemosensitivity in malignant glioma cells. Neurosci Lett 463:54–59

Torsvik A, Stieber D, Enger PO, Golebiewska A, Molven A, Svendsen A, Westermark B, Niclou SP, Olsen TK, Chekenya Enger M, Bjerkvig R (2014) U-251 revisited: genetic drift and phenotypic consequences of long-term cultures of glioblastoma cells. Cancer Med 3:812–824

Uva BM, Masini MA, Sturla M, Bruzzone F, Giuliani M, Tagliafierro G, Strollo F (2002) Microgravity-induced apoptosis in cultured glial cells. Eur J Histochem 46:209–214

Van Ombergen A, Demertzi A, Tomilovskaya E, Jeurissen B, Sijbers J, Kozlovskaya IB, Parizel PM, Van de Heyning PH, Sunaert S, Laureys S, Wuyts FL (2017) The effect of spaceflight and microgravity on the human brain. J Neurol. doi:10.1007/s00415-017-8427-x

Vassy J, Portet S, Beil M, Millot G, Fauvel-Lafeve F, Gasset G, Schoevaert D (2003) Weightlessness acts on human breast cancer cell line MCF-7. Adv Space Res 32:1595–1603

Wang X, Du J, Wang D, Zeng F, Wei Y, Wang F, Feng C, Li N, Dai R, Deng Y, Quan Z, Qing H (2016) Effects of simulated microgravity on human brain nervous tissue. Neurosci Lett 627:199–204

Wang YC, Lu DY, Shi F, Zhang S, Yang CB, Wang B, Cao XS, Du TY, Gao Y, Zhao JD, Sun XQ (2013) Clinorotation enhances autophagy in vascular endothelial cells. Biochem Cell Biol 91:309–314

Wei L, Diao Y, Qi J, Khokhlov A, Feng H, Yan X, Li Y (2013) Effect of change in spindle structure on proliferation inhibition of osteosarcoma cells and osteoblast under simulated microgravity during incubation in rotating bioreactor. PLoS One 8:e76710

Wen PY, Kesari S (2008) Malignant gliomas in adults. N Engl J Med 359:492–507

Xia X, Ma Q, Li X, Ji T, Chen P, Xu H, Li K, Fang Y, Weng D, Weng Y, Liao S, Han Z, Liu R, Zhu T, Wang S, Xu G, Meng L, Zhou J, Ma D (2011) Cytoplasmic p21 is a potential predictor for cisplatin sensitivity in ovarian cancer. BMC Cancer 11:399

Xu H, Wang Z, Jin S, Hao H, Zheng L, Zhou B, Zhang W, Lv H, Yuan Y (2014) Dux4 induces cell cycle arrest at G1 phase through upregulation of p21 expression. Biochem Biophys Res Commun 446:235–240

Zhu M, Jin XW, Wu BY, Nie JL, Li YH (2014) Effects of simulated weightlessness on cellular morphology and biological characteristics of cell lines SGC-7901 and HFE-145. Genet Mol Res 13:6060–6069